



# **Analysis of Flow Conditions in the Stare Miasto Reservoir Taking into Account Sediment Settling Properties**

*Tomasz Dysarz, Joanna Wicher-Dysarz*  
*Poznań University of Life Sciences*

## **1. Introduction**

In this paper the assessment of flow conditions in the Stare Miasto reservoir has been made taking into account the sediment settling properties of the specific construction applied there. The reservoir is split into two parts by an internal dam located in the upper zone. This should protect from fast accumulation of sediment from the area located near the main dam. The analysis has been made on the basis of simulations for selected sets of external flow conditions, such as discharge, water surface head at the main dam and sluice opening.

One of the main problems related to the performance of reservoirs is protection from sediment deposition. Different methods have been applied for this purpose [11, 12]. Very interesting and promising approach seems to be a construction of two-stage reservoir. The main idea of such a solution is to split the reservoir into two parts, namely the main part and the upper sedimentation zone. To achieve this goal, two dams have to be built. The first is the main dam working in the same conditions as in the ordinary single-part reservoir. The second is a smaller dam located in the upper part of the reservoir. The part of the reservoir upstream of this dam is expected to store sediments and pollutants. Such constructions may be found in Poland. An example of a more sophisticated solution is the Mściwojów reservoir [4, 7]. But more direct approaches may also be found, e.g. Poraj reservoir, Kowalskie Lake [9]. New objects of this type are the Roszków reservoir and the Stare Miasto reservoir [9].

The above described construction is based on the observation of natural sedimentation processes in reservoirs. The sediments are deposited first in the upper part of the reservoir near the inlet [11, 12]. The main factor responsible for such distribution of solid particles is a decrease in transport capacity related to a decrease in stream velocity. The most prone to this process are coarser particles. Their deposition on the bottom changes the water levels and inundation frequencies of the floodplains in the backwater part of the inlet. The condition for riparian vegetation growth in this area improve. An example illustrating such relations may be the Jeziorsko reservoir [2, 3, 8].

The finer particles are sediment slower and are transported along the reservoir. Some of them are stopped only at the dam. Only the finest are transported throughout the dam by culverts and spillways [11, 12]. Hence, the idea of a two-stage reservoir with the small upper dam seems to be reasonable.

However, the problem is more complex. The functioning of the internal dam located in the upper part of the object may also cause some problems with local erosion. The scour formation below the dams and weir has been a frequently observed phenomenon. In the reservoir analyzed there is another element that may cause similar effects. This is the highway bridge narrowing the reservoir in the central zone. Hence, the sedimentation process in the Stare Miasto reservoir may have unexpected results.

The main purpose of the presented research is to analyze the flow conditions in the Stare Miasto reservoir. The analysis should bring some expectations on sediment deposition and erosion. The average velocity and the stream power defined by Yang [11, 12] are used. These two parameters are used in the form of dimensionless values related to expressions depending on water surface elevation. The results of calculations are verified by comparison with direct measurements in the reservoir.

The paper consists of 6 sections. The first is the introduction. Then the materials used in our investigation are described. In the third section the methods applied are explained. The results are presented in fourth section. In the fifth one the results are discussed. The conclusions are presented in the last section.

## 2. Materials

### 2.1. The Stare Miasto Reservoir

The Stare Miasto reservoir is located on the Powa river in the central part of Poland. The main dam is located to the south of Konin city. The reservoir is a relatively new object, built in 2006. Its length is 4.5 km and the area of inundation in normal conditions is 90.68 ha. The total capacity of the reservoir is  $2.159 \times 10^6 \text{ m}^3$ , but the capacity used for water supply is  $1.216 \times 10^6 \text{ m}^3$ . Highway A2 is narrowing the active flow cross-section in the central part of the reservoir. The dam splitting the object into the main and upper part is located upstream of the bridge (fig. 1). The upper dam includes a small sluice. The area of the upper part is 27 ha. The capacity of this part is  $0.294 \times 10^6 \text{ m}^3$  [10]. The depth in the reservoir varies from 1.2 m in the upper part to 5.7 m near the main dam.

The upper part of the reservoir plays a specific role. It is used to collect sediment and for water quality protection. It is expected that the sediment transported with the inflowing water is settled in the upper part of the reservoir. After some time the upper part should develop conditions good for vegetation growth. This enables the removal of pollutants from water or their deposition with the sediments.

The Stare Miasto reservoir is multi-purpose and works in the annual cycle. The main part of the reservoir is used in ordinary way. It includes water supply capacity, the dead zone as well as the flood protection capacity and the hydraulic flood protection zone. The water stored is used mainly for irrigation and protection of biological life in the Powa river. An important purpose is the flood protection of Konin city. The reservoir is additionally use for tourism and fishery.

The water surface level varies from the minimum elevation of 92.70 m a.s.l. to 94.00 m a.s.l. Normal water level is 93.50 m a.s.l. [10].

The basic data used for our analyses include the geometry of the reservoir, water surface levels measured in the main dam as well as the inflows to the reservoir. The preparatory data include analysis of measurements and topographic maps in the scale 1:2000 from 2006 [10]. The maps are used for definition of 51 cross-sections from the main dam to Karsy town, where the inflow to the reservoir is located. The distances between the cross-sections vary from 30 to 200 m.

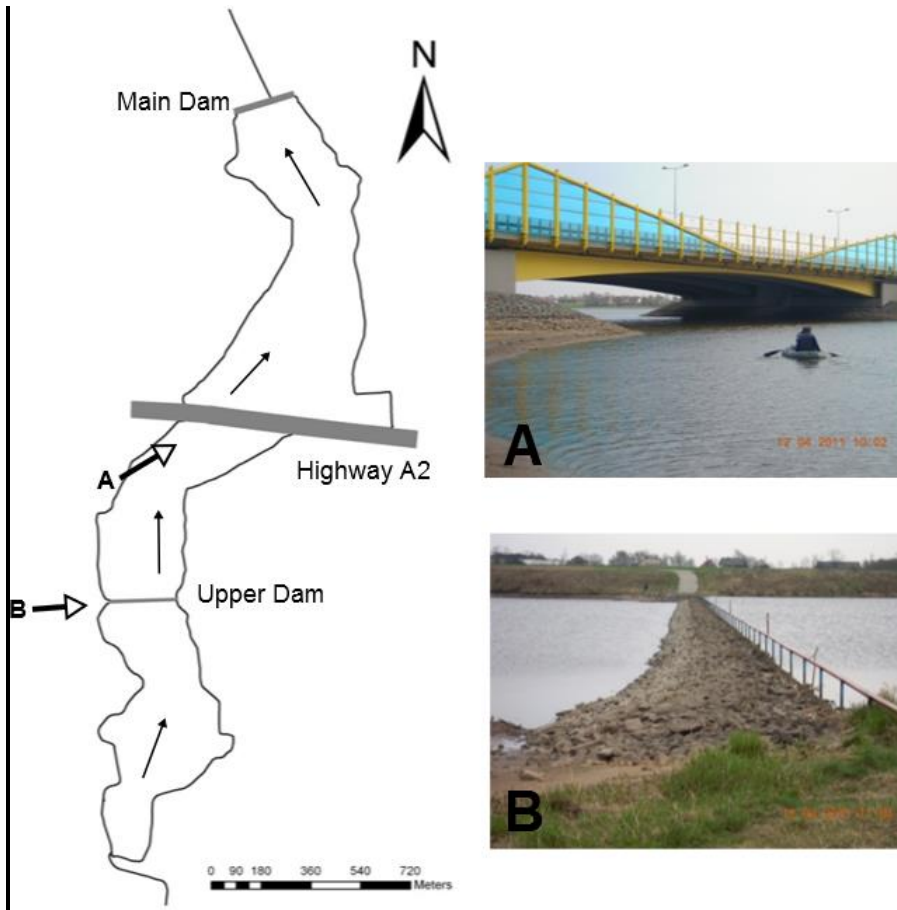


**Fig. 1.** Location of the Stare Miasto reservoir with selected views (Fig. J. Wicher-Dysarz)

**Rys. 1.** Lokalizacja zbiornika Stare Miasto oraz wybrane widoki (Fot. J. Wicher-Dysarz)

The data on discharge observed at the Posoka gauge station in the Powa river are also used. The data from the period 1975 – 2009 are available. The inflow varies from the minimum  $0.012 \text{ m}^3\text{s}^{-1}$  ( $Q_{\text{NNQ}}$ ) to the maximum  $42.6 \text{ m}^3\text{s}^{-1}$  ( $Q_{\text{WWQ}}$ ). The average discharge is  $1.17 \text{ m}^3\text{s}^{-1}$  ( $Q_{\text{SSQ}}$ ). It is important to notice that the average winter discharge is  $1.7 \text{ m}^3\text{s}^{-1}$  and it is significantly greater than the average summer discharge, which is  $0.60 \text{ m}^3\text{s}^{-1}$  [5]. The available data are used for construction of maximum flow curves. The average annual outflow in the period

analyzed was  $36.9 \times 10^6 \text{ m}^3$ . The average annual unit outflow from the watershed is  $3.52 \text{ dm}^3/(\text{km}^2\text{s})$ .

Taking into account the purposes of the analyzes, five discharges are selected. They are presented in tab. 1.

**Table 1** Selected discharges at the cross-section Posoka on the Powa river in the period 1975–2009 [5]

**Tabela 1** Wybrane przepływy dla rzeki Powy w przekroju Posoka w latach 1975–2009 [5]

No.	symbol	meaning	value ( $\text{m}^3/\text{s}$ )
1	$Q_{1\%}$	100-year flow	28.36
2	$Q_{50\%}$	2-year flow	6.87
3	$Q_{SSQ}$	average annual flow	1.17
4	$Q_{SWQ}$	average of maximum flows	8.97
5	$Q_{SNQ}$	average of minimum flows	0.155

### 3. Methods

#### 3.1. Steady flow computations

The computations have been made by application of the well known HEC-RAS package, version 4.1.0. The software consists of several computational modules. For our purposes only the steady flow module is used. It is described below.

The basis for hydraulic computations is the Bernoulli equation

$$H_1 + \alpha_1 \frac{V_1^2}{2g} = H_2 + \alpha_2 \frac{V_2^2}{2g} + \Delta x (\overline{S_f})_{1,2}. \quad (1)$$

In the equation (1),  $H_1$  and  $H_2$  are water surface levels in two particular cross-sections located at sites  $x_1$  and  $x_2$ . These values are the sums of boom elevation and depth according to  $H = z + h$ , where  $h$  represents the pressure head.  $V_1$  and  $V_2$  are average velocities understood as the ratio of discharge  $Q$  and cross-section area  $A$ . In steady flow computations the discharge  $Q$  is constant, but the cross-section area  $A$  is a function of water surface level  $H$ . Parameters  $\alpha_1$  and  $\alpha_2$  are St. Venant coefficients describing the variability of velocity profile in the particular cross-section;  $g = 9.81 \text{ ms}^{-2}$  is acceleration of gravity;  $\Delta x$  is the distance between cross-

sections  $x_1$  and  $x_2$ . The symbol  $(\overline{S_f})_{1,2}$  is the average hydraulic slope along the distance between  $x_1$  and  $x_2$ , which is calculated as basic average of values from cross-sections  $x_1$  and  $x_2$ .

$$(\overline{S_f})_{1,2} = \frac{1}{2}(S_{f1} + S_{f2}), \quad (2)$$

where  $S_{f1}$  and  $S_{f2}$  are hydraulic slopes calculated at sites  $x_1$  and  $x_2$  according to the following formula

$$S_f = n^2 \frac{|Q|Q}{R_h^{4/3} A^2}. \quad (3)$$

The above equation is consistent with the Manning equation. The roughness coefficient is denoted as  $n$ . It is treated as a parameter in particular cross-section. The symbol  $R_h$  is hydraulic radius calculated as the ratio of cross-section area and wetted perimeter. It is a nonlinear function of water surface elevation.

The start of computations is boundary condition applied here as known water surface elevation in the dam cross-section. The cross-sections used for computations are reconstructed from maps. The geometry is completed with two hydraulic structures, namely the highway bridge and the upper dam. A more detailed description of HEC-RAS may be found in Brunner [1].

### 3.2. Prepared computational tests

Twenty 20 computational test were performed and analyzed. They differ in three main elements. These are (1) discharge, (2) water surface elevation in the dam and (3) sluice opening in the upper dam. The simulations are denoted as “testX-Yo”, where “X” is a number from 1 to 5 denoting the discharge tested. These are following discharges  $Q_{1\%}$  (number 1),  $Q_{50\%}$  (2),  $Q_{SSQ}$  (3),  $Q_{SWQ}$  (4) and  $Q_{SNQ}$  (5). The parameter “Y” takes values 1 or 2 corresponding to the normal or minimum water surface elevation in the dam, respectively. The symbol “o” can be replaced by “a” – when the sluice is open, or “b” – when it is closed. For example, “test3-2b” means computations for discharge  $Q_{SWQ}$  with the minimum water level in the main dam and sluice closed in the upper dam. All tested values and notations of calculations are presented in Table 2.

**Table 2.** Description and parameters of calculations at the cross-section Posoka on the Powa river in the period 1975–2009

**Tabela 2.** Opis i parametry obliczeń dla rzeki Powy w przekroju Posoka w latach 1975–2009

No	discharge	dam headwater	sluice opening	description
1	$Q_{1\%} = 28.36 \text{ m}^3\text{s}^{-1}$	normal = 93.50 m a.s.l.	100 %	test1-1a
2			0 %	test1-1b
3		minimum= 92.00 m a.s.l.	100 %	test1-2a
4			0 %	test1-2b
5	$Q_{50\%} = 6.87 \text{ m}^3\text{s}^{-1}$	normal = 93.50 m a.s.l.	100 %	test2-1a
6			0 %	test2-1b
7		minimum= 92.00 m a.s.l.	100 %	test2-2a
8			0 %	test2-2b
9	$Q_{SSQ} = 1.17 \text{ m}^3\text{s}^{-1}$	normal = 93.50 m a.s.l.	100 %	test3-1a
10			0 %	test3-1b
11		minimum= 92.00 m a.s.l.	100 %	test3-2a
12			0 %	test3-2b
13	$Q_{SWQ} = 8.97 \text{ m}^3\text{s}^{-1}$	normal = 93.50 m a.s.l.	100 %	test4-1a
14			0 %	test4-1b
15		minimum= 92.00 m a.s.l.	100 %	test4-2a
16			0 %	test4-2b
17	$Q_{SNQ} = 0.155 \text{ m}^3\text{s}^{-1}$	normal = 93.50 m a.s.l.	100 %	test5-1a
18			0 %	test5-1b
19		minimum= 92.00 m a.s.l.	100 %	test5-2a
20			0 %	test5-2b

### 3.3. Parameters describing flow conditions in the reservoir

The basic parameters describing flow conditions are the water depth and the average velocity along the reservoir. They are presented in fig. 2–6 and fig. 7–8. The more advanced analyzes are made on the basis

of dimensionless parameters. The first is the ratio of velocity head and pressure head defined as follows

$$VP = \frac{V^2}{2gh}, \quad (4)$$

where  $h$  is the difference between water surface elevation and minimum bottom elevation at a particular cross-section. These values are presented in fig. 9–10.

The second parameter is based on the stream power used as a basis in the Yang (1973) method. The stream power is a product of shear stress and velocity

$$SP = \tau V, \quad (5)$$

expressed in N/(ms). Shear stress is calculated as follows

$$\tau = \rho g R_h S_f, \quad (6)$$

in  $\text{Nm}^{-2}$ .

The dimensionless stream power is defined here as the ratio of (5) to average pressure at a cross-section and velocity recalculated into water depth according to the Torricelli formula. It is written below

$$SPD = \frac{\tau}{\left(\frac{1}{2}\rho gh\right)} \frac{V}{\sqrt{2gh}} = \frac{\sqrt{2}}{\rho(gh)^{3/2}} \tau V, \quad (7)$$

where  $\rho$  is water density.

### 3.4. Direct measurements of cross-sections

The last element of the method applied are direct measurements of reservoir cross-sections. Such a survey was made in August 2011. The measurements were made on the river reach along the length of 3.5 km from the main dam to the reservoir inlet in Karsy town. The field survey was made using a standard GPS unit and an acoustic Doppler current meter. The GPS used was able to measure the position as well elevations. The applied current meter was StreamPro ADCP (Acoustic Doppler Current Meter) produced by Teledyne RD Instruments. This device was used for measurements of flow velocity as well as the reservoir depth.

Measurements were made at 21 cross-sections at distances varying from 100m to 200 m. The water surface elevation was also measured. Three cross-sections shown in fig. 13-15 were used for comparisons with historical cross-sections.

## 4. Results

### 4.1. Water surface profiles

The main results are presented as water surface profile along the reservoir. It was noticed that the sluice is opening is not so important as other factors, i.e. discharge and water surface at the main dam. Hence, only the results of the tests with full opening are presented, see fig. 2–6.

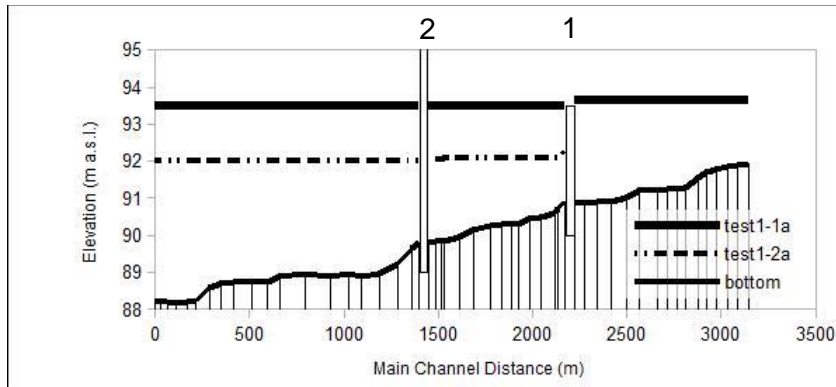


**Fig. 2.** Water table profiles for  $Q_{1\%} = 28.36 \text{ m}^3\text{s}^{-1}$  with normal (93.50 m a.s.l., test1-1a) and minimum (92.00 m a.s.l., test1-2a) water surface elevation at the dam (1 - upper dam, 2 – highway A2)

**Rys. 2.** Profil zwierciadła wody dla  $Q_{1\%} = 28.36 \text{ m}^3\text{s}^{-1}$  z normalnym (93.50 m n.p.m., test1-1a) i minimalnym (92.00 m n.p.m., test1-2a) poziomem piętrzenia na zaporze (1 – przegroda, 2 – autostrada A2)

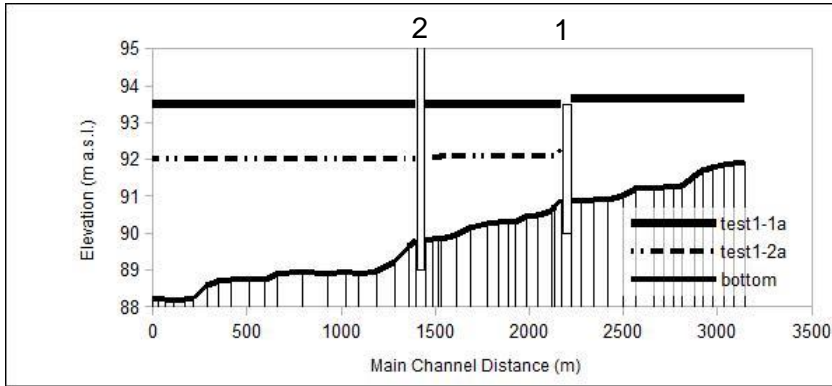


**Fig. 3.** Water table profiles for  $Q_{50\%} = 6.87 \text{ m}^3\text{s}^{-1}$  with normal (93.50 m a.s.l., test2-1a) and minimum (92.00 m a.s.l., test2-2a) water surface elevation at the dam (1 - upper dam, 2 – highway A2)

**Rys. 3.** Profil zwierciadła wody dla  $Q_{50\%} = 6.87 \text{ m}^3\text{s}^{-1}$  z normalnym (93.50 m n.p.m., test2-1a) i minimalnym (92.00 m n.p.m., test2-2a) poziomem piętrzenia na zaporze (1 – przegroda, 2 – autostrada A2)

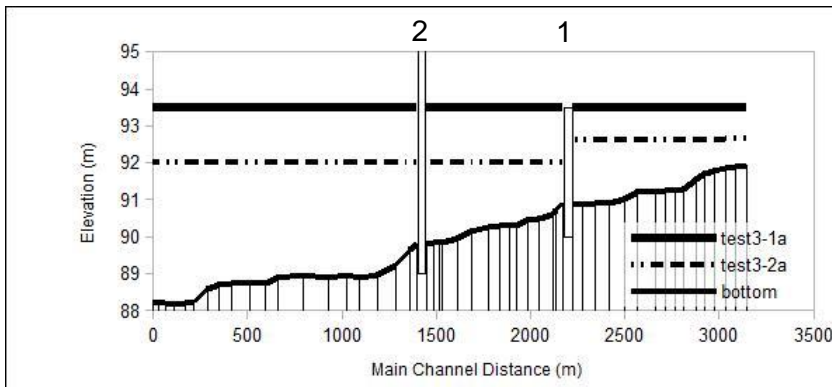


**Fig. 4.** Water table profiles for  $Q_{SSQ} = 1.17 \text{ m}^3\text{s}^{-1}$  with normal (93.50 m a.s.l., test3-1a) and minimum (92.00 m a.s.l., test3-2a) water surface elevation at the dam (1 - upper dam, 2 – highway A2)

**Rys. 4.** Profil zwierciadła wody dla  $Q_{SSQ} = 1.17 \text{ m}^3\text{s}^{-1}$  z normalnym (93.50 m n.p.m., test3-1a) i minimalnym (92.00 m n.p.m., test3-2a) poziomem piętrzenia na zaporze (1 – przegroda, 2 – autostrada A2)

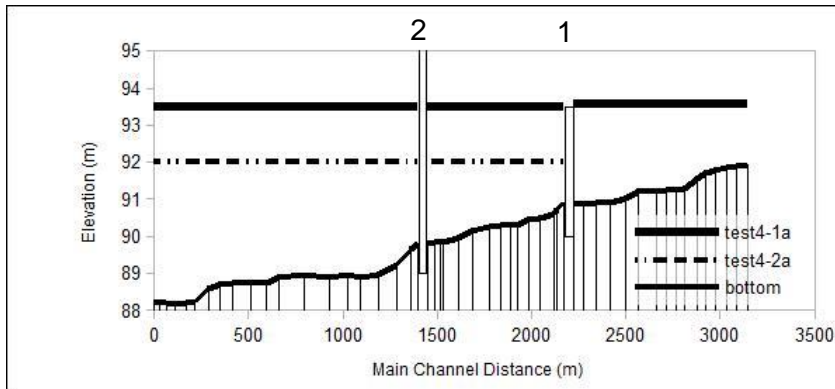


**Fig. 5.** Water table profiles for  $Q_{SWQ} = 8.97 \text{ m}^3\text{s}^{-1}$  with normal (93.50 m a.s.l., test4-1a) and minimum (92.00 m a.s.l., test4-2a) water surface elevation at the dam (1 – upper dam, 2 – highway A2)

**Rys. 5.** Profil zwierciadła wody dla  $Q_{SWQ} = 8.97 \text{ m}^3\text{s}^{-1}$  z normalnym (93.50 m n.p.m., test4-1a) i minimalnym (92.00 m n.p.m., test4-2a) poziomem piętrzenia na zaporze (1 – przegroda, 2 – autostrada A2)

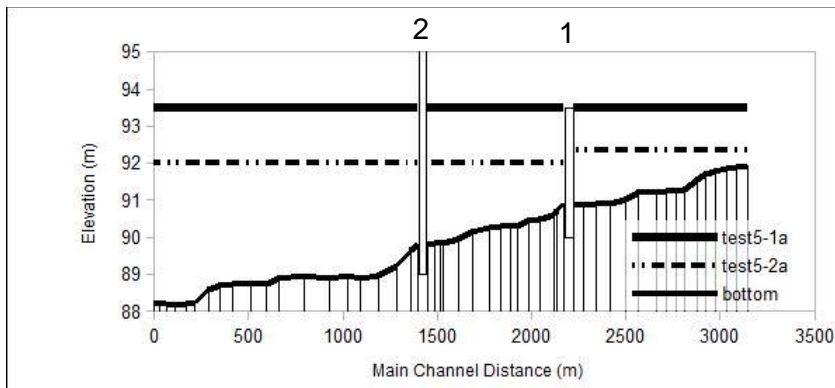


**Fig. 6.** Water table profiles for  $Q_{SNQ} = 0.155 \text{ m}^3\text{s}^{-1}$  with normal (93.50 m a.s.l., test5-1a) and minimum (92.00 m a.s.l., test5-2a) water surface elevation at the dam (1 – upper dam, 2 – highway A2)

**Rys. 6.** Profil zwierciadła wody dla  $Q_{SNQ} = 0.155 \text{ m}^3\text{s}^{-1}$  z normalnym (93.50 m n.p.m., test5-1a) i minimalnym (92.00 m n.p.m., test5-2a) poziomem piętrzenia na zaporze (1 – przegroda, 2 – autostrada A2)

In figs. 2–6, the horizontal axis represents the distance measured from the main dam. The elevations of water surface and bottom are shown on the vertical axis. In all figures, the bottom profile is the lowest thin and continuous line. The ground is the area below this line drawn as vertical sections reaching the bottom line. The water elevation calculated for normal head at the main dam is the highest thick and continuous line. The water level calculated for the minimum head at the main dam is denoted as dots and broken line.

The bridge and the upper dam are also marked in the figures. The first is the higher vertical rectangle on the left. The invert of this rectangle extends beyond the figure, because the upper elevation of the bridge is greater than the elevation scale. The second rectangle on the right is smaller and represents the upper dam.

#### **4.2. Velocity distribution**

The next results presented are average velocity distributions along the reservoir. The results of selected tests are shown in fig. 7–8. As previously, the horizontal line represents the distance from the main dam, while the vertical line shows velocity. The bridge and the upper dam dividing the reservoir are marked as gray vertical lines. The velocity distributions are presented as different lines described in the legend. The calculations with normal water surface head at the main dam are shown in fig. 7. The second figure (fig. 8) is presents the results obtained for minimum water level at the main dam.

#### **4.3. Ratio of velocity head and pressure head**

The results in fig. 7–8 are not clear enough to reveal some important dependencies and patterns in flow condition changes along the reservoir. Hence, the results obtained are also presented by means of parameters defined by (4) and (7). The ratio of velocity head to pressure head is presented in fig. 10–11. The distance from the dam is represented on the horizontal axis. The vertical axis shows logarithms of (4). The bridge and the upper dam are marked as gray vertical lines. The results of different tests are presented as lines described in the legend. The calculations with normal water surface head at the main dam are shown in fig. 9. The second figure (fig. 10) presents the results obtained for minimum water level at the main dam.

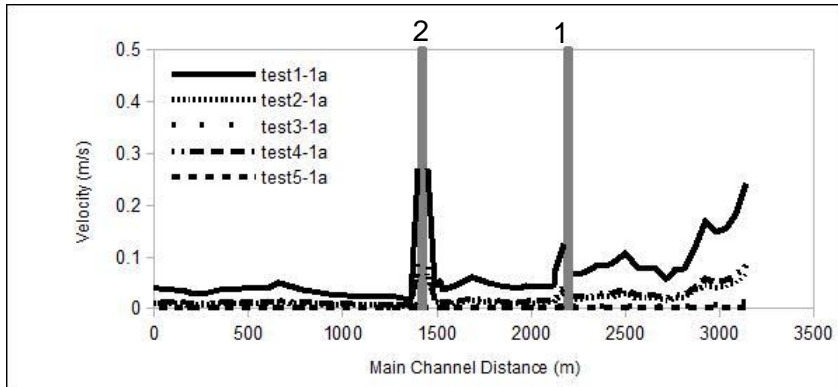


**Fig. 7.** Velocity distribution for tests with normal (93.50 m a.s.l.) water surface elevation at the dam (1 – upper dam, 2 – highway A2)

**Rys. 7.** Rozkład prędkości w testach z normalnym (93.50 m n.p.m.) poziomem piętrzenia na zaporze (1 – przegroda, 2 – autostrada A2)

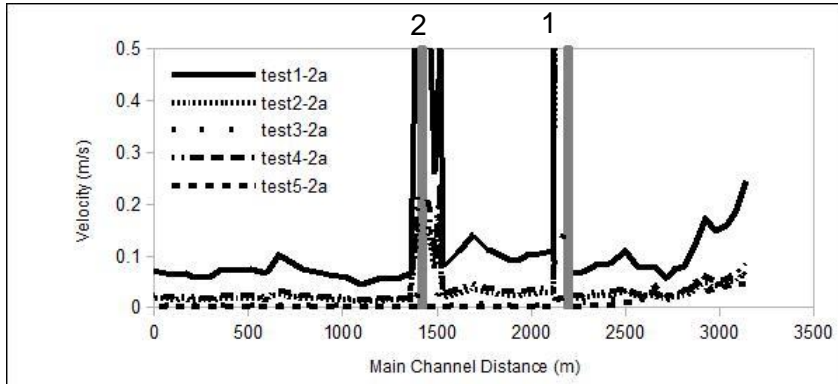


**Fig. 8.** Velocity distribution for tests with minimum (92.00 m a.s.l.) water surface elevation at the dam (1 – upper dam, 2 – highway A2)

**Rys. 8.** Rozkład prędkości w testach z minimalnym (92.00 m n.p.m.) poziomem piętrzenia na zaporze (1 – przegroda, 2 – autostrada A2)

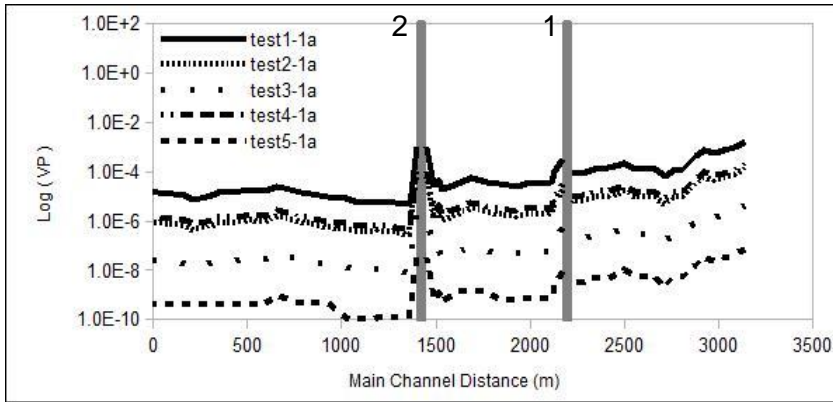


**Fig. 9.** Ratio of velocity head and pressure head for tests with normal (93.50 m a.s.l.) water surface elevation at the dam (1 – upper dam, 2 – highway A2)

**Rys. 9.** Stosunek wysokości prędkości do wysokości ciśnienia w testach z normalnym (93.50 m n.p.m.) poziomem piętrzenia na zaporze (1 – przegroda, 2 – autostrada A2)

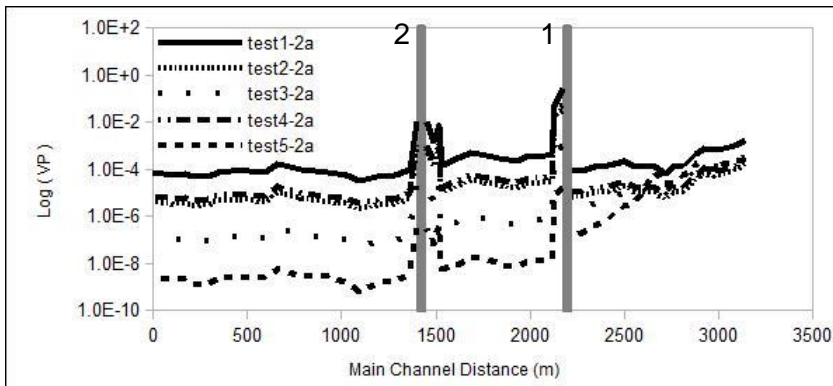


**Fig. 10.** Ratio of velocity head and pressure head for tests with minimum (92.00 m a.s.l.) water surface elevation at the dam (1 – upper dam, 2 – highway A2)

**Rys. 10.** Stosunek wysokości prędkości do wysokości ciśnienia w testach z minimalnym (92.00 m n.p.m.) poziomem piętrzenia na zaporze (1 – przegroda, 2 – autostrada A2)

#### 4.4. Dimensionless stream power

The fig. 11–12 present the results of simulation as distribution of dimensionless stream power defined by (7). The denotations are the same as in fig. 9–10, with two exceptions. The first are the values represented in the vertical axis. This time they are logarithms of (7). The second exception is the lack of results from “test5-1a” in fig. 11. They have been omitted because of too small values.

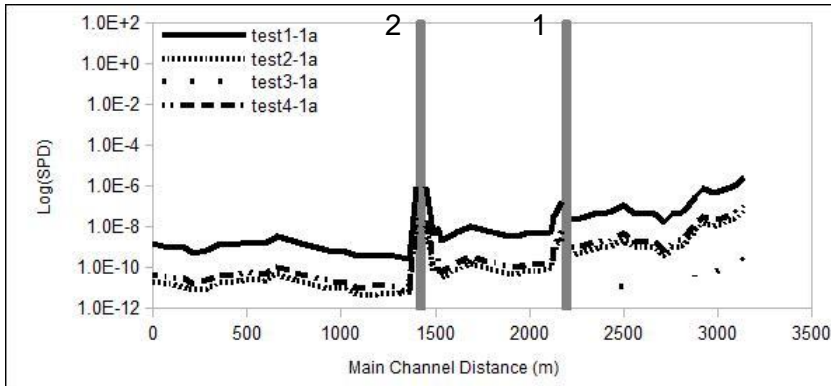


**Fig. 11.** Dimensionless stream power for tests with normal (93.50 m a.s.l.) water surface elevation at the dam (1 – upper dam, 2 – highway A2)

**Rys. 11.** Bezwymiarowa moc strumienia w testach z normalnym (93.50 m n.p.m.) poziomem piętrzenia na zaporze (1 – przegroda, 2 – autostrada A2)

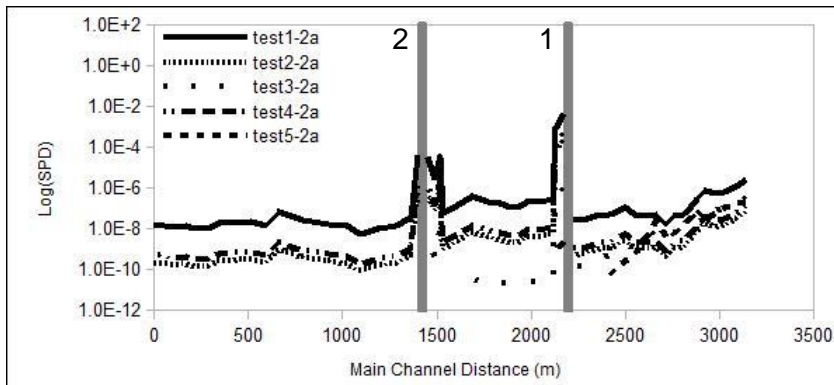


**Fig. 12.** Dimensionless stream power for tests with minimum (92.00 m a.s.l.) water surface elevation at the dam (1 – upper dam, 2 – highway A2)

**Rys. 12.** Bezwymiarowa moc strumienia w testach z minimalnym (92.00 m n.p.m.) poziomem piętrzenia na zaporze (1 – przegroda, 2 – autostrada A2)

#### 4.5. Direct comparison of cross-sections

A comparison of historical and calculated cross-sections in the reservoir is shown in fig. 13–15. The results are presented for three cross-sections selected in such a way that the most important changes are pronounced. The first cross-section, shown in fig. 13, is located just downstream of the bridge. The second cross-section is presented in fig. 14. It is below the upper dam. The third cross-section (fig. 15) shows the changes in the upper part of the reservoir.

In fig. 13–15, the horizontal axis represent distance measured along the cross-section. The vertical axis shows the elevations above sea level. The thick continuous and horizontal line is normal water table. The thin line represents the designed cross-section shape. The crosses are measured ground level in the year 2011.

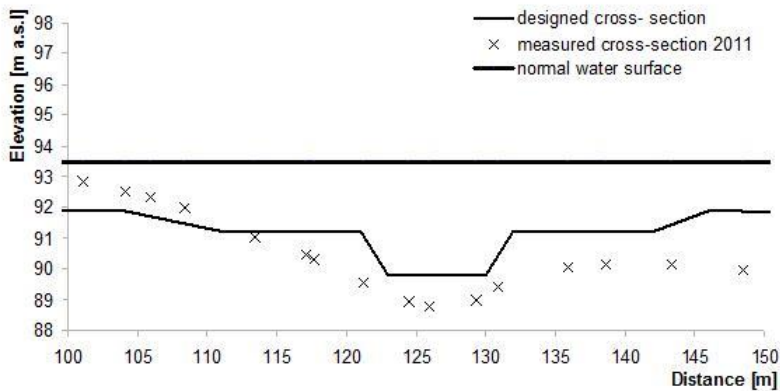


**Fig. 13.** Comparison of measured and calculated cross-section shape downstream of the bridge

**Rys. 13.** Porównanie pomierzonego i obliczonego kształtu przekroju poprzecznego poniżej mostu

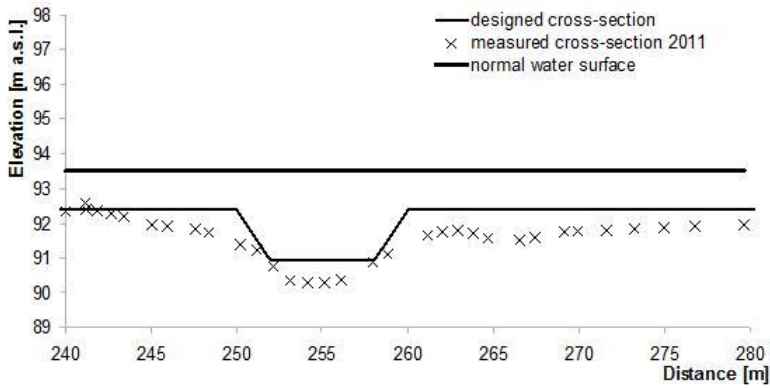


**Fig. 14.** Comparison of measured and calculated cross-section shape downstream of the upper dam

**Rys. 14.** Porównanie pomierzonego i obliczonego kształtu przekroju poprzecznego poniżej górnej zapory

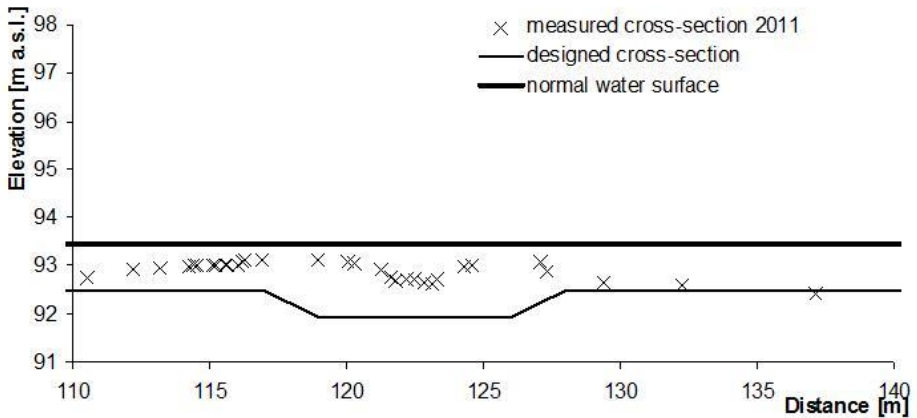


**Fig. 15.** Comparison of measured and calculated cross-section shape in the upper part of the reservoir

**Rys. 15.** Porównanie pomierzonego i obliczonego kształtu przekroju poprzecznego w górnej części zbiornika

## 5. Discussion

The relation between the computations performed and the real conditions in the Stare Miasto reservoir is the first concern in the discussion of results. The tested discharges presented in tab. 2 seem to cover the main range of discharge variability in the analyzed reservoir. The minimum and normal water surface elevations at the main dam reflect also the most typical conditions of reservoir performance. Hence, the presented tests appear to be proper for the assessment of flow conditions in the object analyzed.

The fundamental results are water surface profiles presented in fig. 2–6. Results of the computations indicated small influence of the fact whether the sluice was open or closed on the water surface profile along the reservoir. The main factor determining such a profile is the water surface head imposed at the main dam and used as boundary condition in computations. Hence, only the results of selected tests are presented in fig. 2–6. These are tests with sluice fully opened. The water surface in the upper part of the reservoir is kept on the same or similar level as the water surface in the lower part if normal water surface elevation at the main dam is tested. The higher water level in the upper part is only noticed in the results of the first test for the greatest discharge, which equals  $Q_{1\%} = 28.36 \text{ m}^3\text{s}^{-1}$ . Otherwise, the reason for such high water level in the upper part is the elevation of the upper dam crest. This exactly equals the normal water surface elevation. If the imposed water table at the main dam is taken as minimum water level, the water elevations in the lower and upper part of the reservoir may differ. But, the difference decreases with decreasing discharge tested. It suggests that the main factor influencing this difference is the capacity of the sluice in the upper dam.

The results presented in fig. 7–8 show distribution of average velocity along the reservoir. The same tests are analyzed, which results are shown in fig. 2–6. It is noticed that the velocity decreases quickly in the upper part of the reservoir irrespective of the conditions analyzed. The decrease is greater for greater discharges. It should suggest that the stream capacity of sediment is gradually decreasing in the upper part. In the lower part the velocity seems to be more or less constant. The value of flow velocity depends on the discharge. The exception from this pat-

tern are relatively small zones near the upper dam and the bridge. In these parts the velocity increases rapidly, which favors local erosion.

In general, the results presented in fig. 7–8 are not very clear because of the scale used. It is the reason for use of dimensionless parameters defined by (4) and (7). They are presented in semi-logarithmic scale, which improves the meaning of the next graphs.

The ratio of velocity head and pressure head (4) is presented in fig. 9–10. The results confirm the previous remarks. In the case of normal water surface level in the main dam the distribution of (4) directly depends on the discharge. In the case of minimum water surface level, the patterns presented in fig. 10 are more complex. It is directly related to the dependence of water surface profile on discharge. The values of (4) decrease gradually in the upper part of the reservoir. They are smaller and relatively constant in the lower part of the object. The rapid increases in (4) are noticed near the upper dam and the bridge. They are very similar to the increases of velocity shown in fig. 7–8.

The dimensionless stream power presented in the semi-logarithmic scale in fig. 11–12 shows a gradual decrease in the upper part of the reservoir and relatively constant values in the rest of the object. The decrease is greater for the normal water surface level imposed at the main dam. The greater deposition should be observed there. Rapid changes in (7) are noticed near the upper dam and the bridge. It is expected to observe erosion changes below these two structures. In general, the results in fig. 11–12 confirm the previous remarks.

The last results presented are comparisons of designed and current cross-sections. They are shown in fig. 13–15. The first cross-section (fig. 13) is located downstream of the bridge. The difference between designed cross-section shape (continuous line) and measurements made in 2011 (crosses) confirms the expectations formulated on the basis of analyzes presented in previous figures. Rapid increases in velocity as well as dimensionless parameters (4) and (7) indicate that erosion should be observed below the bridge. The second cross-section (fig. 14) is located downstream of the upper dam. The graph confirms similar expectations as predicted near the bridge. The last cross-section (fig. 15) is located near the inlet to the upper part of the reservoir. In this area deposition is expected, as also indicated in fig. 15.

## 6. Conclusions

The main purpose of the paper is analysis of flow conditions in the Stare Miasto reservoir. The analysis has been made taking into account the potential sediment deposition and erosion along the reservoir. The importance of the presented consideration is related to the specific construction of the reservoir. This is a two-stage object with the main dam and the upper dam constraining the upper sedimentation zone. The problem becomes more complex because of the influence of the highway bridge, which has narrowed the central part of the reservoir.

The main tool used for the assessment is HEC-RAS package. The results of the calculations are analyzed as water surface profiles and velocity distribution along the reservoir. The need for clear presentation of results has led to some dimensional parameters. The expressions applied are the ratio of velocity head to pressure head defined by (4) and dimensionless stream power (7). These tools enabled proper identification of sediment deposition zones as well as the local erosion places. The comparison of calculation results with direct measurements has confirmed our observations.

The calculations showed that the two-stage construction of the reservoir seems to perform well. The sediment particles are settled in the upper part of the reservoir as expected. However, the flow conditions presented indicate also some problems which were not predicted earlier. There are some sites at which local erosion may occur. The first is the cross-section downstream of the upper dam. Such problems have to appear if two-stage construction of the reservoir is applied. The second site is located downstream of the highway bridge. Another problem is the constraint on active flow area caused by the bridge. It appears that flow conditions were not taken into account when the bridge was designed. Today it may cause huge problems.

The computations performed enabled proper identification of deposition zone as well as the cross-sections prone to erosion. The comparison of selected cross-sections with direct measurements verify the conclusions presented. The parameters applied, VP and SPD may be recommended for application in design of reservoirs in future.

*This work is a part of a scientific project "Initial sedimentation part in small lowland reservoirs: modelling and analysis of functionality" founded by National Science Centre in Poland, no. N N305 296740*

## References

1. **Brunner G.W.:** *HEC-RAS, River Analysis System, Hydraulic Reference Manual*. Davis, CA.: US Army Corps of Engineers, Hydrologic Engineering Center, 2010.
2. **Dysarz T., Wicher-Dysarz J.:** *Application of hydrodynamic simulation and frequency analysis for assessment of sediment deposition and vegetation impacts on floodplain inundation*. Polish Journal of Environmental Studies Vol. 20, No 6 (2011), 1441–1451.
3. **Dysarz T., Wicher-Dysarz J., Przedwojski B.:** *Man-induced morphological processes in Warta river and their impact on the evolution of hydrological conditions*, in Ferreira R.M.L., Alves E.C.T.L., Leal J.G.A.B., Cardoso A.H. (eds.): *River Flow 2006*, Taylor & Francis Group, 1301–1310 (2006).
4. **Kasperek R., Wiatkowski M.:** *Research on bottom sediments from the Mściwojow reservoir*. (in Polish), *Przegląd Naukowy Inżynieria i Kształtowanie Środowiska*, 40, 194–201 (2008).
5. **Matuszewski Sz.:** *One-dimensional modeling of the hydrodynamics and sediment transport in the Stare Miasto reservoir*. Maszynopis pracy mgr, promotor J. Wicher-Dysarz, UP Poznań, 2012.
6. **Morris G.L., Fan J.:** *Reservoir sedimentation Handbook*. McGraw-Hill, 2009.
7. **Pikul K., Mokwa M.:** *Influence of pre-dam reservoir on sedimentation process in main reservoir*, *Przegląd Naukowy Inżynieria i Kształtowanie Środowiska*, 40, 185–193 (2008).
8. **Walczak N., Walczak Z.:** *Assessment of vegetation impact on velocity distribution on the basis of field measurements in the Warta river (in Polish)*, *Gospodarka Wodna*, 1/2011 449–453 (2011).
9. **Wicher-Dysarz J., Kancelrz J.:** *Functioning of small lowland reservoirs with pre-dam zone: the Kolwalskie Lake and the Stare Miasto Reservoirs case studies*, *Rocznik Ochrona Środowiska (Annual Set The Environment Protection)*, 14, 2012 (in Polish).
10. **Woliński J., Zgrabczyński J.:** *The Stare Miasto reservoir in the Powa river: Water management rules*, *Biuro Projektów Wodno Melioracyjnych „BIPROWODMEL” Sp. z o.o Poznań 2008*.
11. **Yang C.T.:** *Incipient Motion and Sediment Transport*, *Journal of Hydraulic Division, American Society of Civil Engineers*, Vol. 99, No HY10, October, 1973, 1679–1704 (1973).
12. **Yang C.T.:** *Sediment transport theory and practice*. McGraw-Hill Series in Water Resources and Environmental Engineering, 1996.

## **Analiza warunków przepływu w zbiorniku Stare Miasto z uwzględnieniem właściwości osadów**

### **Streszczenie**

W przedstawionym artykule analizowane są warunki przepływu w zbiorniku wodnym Stare Miasto. Analizy uwzględniają wpływ parametrów hydraulicznych na rodzaj procesów sedymentacyjnych i erozyjnych w zbiorniku. Obiekt wybrano ze względu na jego specyficzną konstrukcję. Jest to zbiornik dwustopniowy. Górna część jest oddzielona od głównego zbiornika przegrodą z przelewem zastawkowym. Dzięki takiemu układowi, w górnej części tworzą się warunki dogodne do tworzenia odkładów rumowiska. Jednak istnienie dodatkowych konstrukcji, takich jak przegroda i most autostrady A2, mogą zaburzyć przebieg procesu transportu rumowiska tworząc lokalne efekty erozyjne.

W badaniach posłużono się zgromadzonymi materiałami obejmującymi geometrię czaszy zbiornika, wymiary uwzględnionych budowli, hydrologię oraz zakres piętrzeń na zaporze. Analizy przeprowadzono na podstawie obliczeń symulacyjnych wykonanych za pomocą programu HEC-RAS. W analizach zwrócono uwagę na rozkłady prędkości oraz tzw. moc strumienia będącą podstawą metody Yanga (1973). W celu lepszego przedstawienia wyników zdefiniowano miary bezwymiarowe będące odpowiednikami analizowanych wielkości. Wyniki analiz zweryfikowano poprzez porównanie historycznego kształtu wybranych przekrojów z pomierzonymi przekrojami dna zbiornika.

Zastosowane metody pozwoliły wiarygodnie zidentyfikować miejsca zwiększonego deponowania rumowiska oraz erozji. Konstrukcja dwustopniowa spełnia swoje zadanie, tzn. większość rumowiska powinna być zatrzymywana przez górną przegrodę.